Anion Uptake in Halorhodopsin from *Natromonas pharaonis* Studied by FTIR Spectroscopy: Consequences for the Anion Transport Mechanism†

Jarmila Guijarro,‡,|| Martin Engelhard,§ and Friedrich Siebert*,‡

Sektion Biophysik, Institut für Molekulare Medizin und Zellforschung, Albert-Ludwigs-Universität, 79104 Freiburg, Germany, and Max-Planck-Institut für Molekulare Physiologie, 44227 Dortmund, Germany

Received April 19, 2006; Revised Manuscript Received June 24, 2006

ABSTRACT: The uptake of chloride, bromide, iodide, nitrate, and azide by anion-depleted blue halorhodopsin from *Natronobacterium pharaonis* has been followed by FTIR difference spectroscopy using an ATR sampling device. The spectra are compared with the spectrum of the O intermediate obtained by time-resolved FTIR studies of the photocycle. It is demonstrated that anion-free blue halorhodopsin can be identified with the O intermediate and, thus, that the decay of O is due to the passive uptake of the anion. The great similarity of the anion-binding spectra and their identity in the case of the monoatomic anions indicate a rather unspecific binding site for the different anions dominated by electrostatic interactions. Comparing spectra obtained with ^{15}N nitrate and unlabeled nitrate, the NO-stretching bands could be identified. The small splitting and the small IR intensity of those bands indicate a rather nonpolar binding site with a rather isotropic influence on the nitrate, in contrast to aqueous nitrate. In further experiments on the photocycle of blue halorhodopsin, the all-trans → 13-cis isomerization can be clearly identified. Up to 100 μs, the isomerization-induced structural changes deduced from amide I changes are similar to those occurring during the anion-transporting photocycle. Compared to these, the molecular changes involved in the release and their reversion during the uptake of anions are considerably larger. They can be reached via two pathways: (1) by reducing the anion concentration and (2) transiently during the anion-transporting photocycle with the formation of the precursor of O with O conformation. Consequences of the anion transport mechanism are discussed.

Although the structure of the light-driven anion pump halorhodopsin from *Halobacterium salinarum* (HsHR[1]) has been determined (*1*), the mechanism of anion transport in this system from the extracellular medium into the cytoplasm, against a gradient, still represents a puzzle. Halorhodopsin from *Natronobacterium pharaonis* (*2*) (NpHR) shares considerable homology with HsHR, which argues for a similar if not identical anion-translocating mechanism triggered by the photoisomerization of the all-trans retinal to the 13-cis form. Despite these similarities, there are, as detailed later, pronounced differences in anion specificity and affinity. In addition, whereas the isomeric composition in the dark state is similar in the two systems, in NpHR, only that part containing the all-trans chromophore undergoes a photocycle, in contrast to HsHR (*3*). When comparing functionally important residues of halorhodopsin with those of the related light-driven proton pump bacteriorhodopsin (BR), one of the striking differences concerns the counterion of the protonated Schiff base in BR, Asp85, which is replaced by a threonine (Thr111 in HsHR and Thr126 in NpHR). Interestingly, if Asp85 in BR is mutated to a threonine, then the proton pumping capability is abolished and a light-activated chloride pump is obtained (*4*, *5*). The photocycles of the Asp85Thr and Asp85Ser mutants of BR and of HsHR bear some resemblance to each other; however the former exhibits a 20-fold smaller chloride affinity (*5*, *6*). A common feature of the photocycles of the BR mutant and of both halorhodopsins is that no deprotonation of the Schiff base takes place. It is, therefore, probable that the anions are bound at comparable protein sites like the protonated Schiff base and Thr85. There have been controversial reports on the number of anion binding sites and their role in anion pumping spectroscopic studies (see ref *7*−*12* and references cited in ref *7*) and transport investigations (*13*−*15*). Furthermore different results were obtained for HsHR and NpHR. Arg200 and Thr203 have been identified to be important for the release site in HsHR (*16*), and similar conclusions have been reached for the corresponding residues Lys215 and Thr218 in NpHR (*11*). When adding a second-site mutation in the cytoplasmic channel of the Asp85Thr mutant of BR, a specific influence of Thr178 on the chloride dependence of the kinetics forming an O-like intermediate could be demonstrated (*6*). Thr178 corresponds to Thr218 in NpHR. This analogy provides an indication for the close relationship between the proton- and chloride-pumps.

† This work was supported by Deutsche Forschungsgemeinschaft Grant SI 278/23-1,2 to F.S.

* Corresponding author. Tel. +49-761-203-5396. Fax: +49-761-203-5390. E-mail: frisi@biophysik.uni-freiburg.de.

‡ Albert-Ludwigs-Universität.

§ Max-Planck-Institut für Molekulare Physiologie.

|| Present address: Institut für Chemie, Max Volmer Laboratorium, Technische Universität Berlin, 10623 Berlin, Germany.

[1] [1]Abbreviations: ATR, attenuated total reflection; BR, bacteriorhodopsin; FTIR, Fourier transform infrared; K, L1, L2, O, intermediates of the photoreaction of halorhodopsin; MOPS, (3-[*N*-morpholine]-propanesulfonic acid); NpHR, halorhodopsin from *Natronobacterium pharaonis*; HsHR, halorhodopsin from *Halobacterium salinarum*; NpHR576, initial (dark) state of NpHR.

10.1021/bi060753j CCC: $33.50
Published on Web 08/29/2006

The crystal structure of HsHR revealed the complex nature of the chloride binding close to the Schiff base, indicating the participation of several side chains and two crystallographic water molecules (*1*). Surprisingly, it is not the OH group of T111 that is involved in chloride binding but the $-CH_3$ group. Electrostatic calculations seem to support the distributed role of the groups for chloride binding (*1*), which also include aliphatic hydrogens. With respect to the release site, a possible role of T203 seems to be supported by the structure. The cytoplasmic channel appears quite closed, probably requiring conformational changes to allow for the passage of the anion. Therefore, it is not surprising that no chloride could be detected in this channel. Time-resolved UV−vis (*17*) and FTIR (*18*) studies indicated in O a release site with very low affinity (around 4 M), which would be in agreement with the supposition that the chloride is transferred into the cytosol via diffusion (*11*).

If NpHR is suspended in a medium without anions, the color changes to blue, indicating the shift of the absorption maximum from 576 nm (in the presence of chloride) to 600 nm (anion-free) (*19*). The purple to blue shift is explained by the removal of the anion from its binding site close to the Schiff base (i.e., by removal of the counterion). Thus, blue NpHR represents an anion-free state. Also, pH has some influence on the absorption maximum, both in the purple and blue forms with lower pH inducing a blue shift (*19*). Because the shifts are induced by high salt concentrations, these seem to reflect more indirect effects on the protein. Besides the physiological transported anion chloride, bromide, iodide, and nitrate are also pumped. In contrast to HsHR, the latter is pumped by NpHR as efficiently as chloride (*2*). This has been recently confirmed by time-resolved UV−vis and electrical measurements, and it has been concluded that the energetics are very similar to that of NpHR containing chloride (*20*). In the anion-transporting photocycle of NpHR, at least four intermediates have been identified, appearing in the order K, L1, L2 (N), and O. The L1 → L2 transition is a so-called spectrally silent transition, involving only changes of the protein, not of the chromophore. It is often proposed that in this step, the anion is transferred from one side of the Schiff base to the other (*17*, *18*). It is generally assumed that an anion-free state also occurs during this photocycle, that is, when the anion has been released to the cytosolic side of the membrane and not yet taken up from the extracellular side. Most models assume that the O intermediate represents this state, mainly because it also exhibits a red-shifted absorption maximum and because the decay of O is slowed down by reducing the chloride concentration, as expected for a bimolecular reaction (*18*, *21*). Time-resolved electric measurements indicate that the largest charge movement takes place between the L2 (N) and O intermediates, which is interpreted as the movement of the anion from a position still close to the Schiff base to the release site and/or to the cytosolic phase. However, the reformation of the initial state is not connected with a large charge movement, indicating that the anion binds close to the extracellular surface of NpHR (*22*).

A recent crystal structure of the L1 photoproduct of HsHR trapped at low temperature became available (J. Tittor, personal communication). In this state, a small movement of the anion could be detected 0.7 Å away from the Schiff base. However, resonance Raman (*23*) and our own low-temperature FTIR studies (*18*) of NpHR revealed an influence of the type of bound anion on the C=N stretch of the protonated Schiffe in L1 but not in NpHR576, the initial state of NpHR. It was concluded that in L1, the anion moves closer to the Schiff base. Thus, if the interpretation of the spectroscopic data is correct, then the early molecular events must be different in NpHR compared to those in HsHR. Nevertheless, in L1 of both systems, the anion is still close to the Schiff base.

The influence of different anions on the retinal binding site has been studied using low-temperature FTIR spectroscopy on the transitions to K and L1 (*24*). An influence on water molecules and on the NH-stretching mode of the protonated Schiff base has been deduced. The latter result seems to be at variance with the insensitivity of the C=N stretch to the type of anion (*23*). In addition, the variation of the C=C stretch in L1 with the kind of anion is difficult to reconcile with the conclusions from the FTIR experiments, which idicate that in L1 the interaction of the protonated Schiff base with the anions is reduced.

The aim of our studies is to characterize the molecular events involved in anion uptake, both during the photocycle and in the transition from the static anion-depleted form (blue NpHR) to the anion-bound form (NpHR576). For this purpose, we compare the previously obtained time-resolved FTIR difference spectra of the photocycle in the presence of anions with static FTIR difference spectra obtained by the titration of blue NpHR with different anions. The vibrational modes of nitrate are used to monitor its interaction with the protein. We further compare the time-resolved FTIR difference spectra of the pumping-inactive photocycle of blue NpHR with those of the active photocycle. The results clearly demonstrate the role of a negative charge (the anion) at the primary binding site for directing the light-induced molecular changes into a photocycle capable of ion translocation. Interestingly, it is not the retinal isomerization but the release respective uptake of the anion that causes larger changes in the spectra and, therefore, reflects larger protein changes. The results are discussed in the context of a suggested mechanism of anion translocation.

MATERIALS AND METHODS

Preparation of Halorhodopsin Samples. NpHR expressed in *E. coli* was prepared as described by Hohenfeld et al. (*25*). To simulate the physiological membrane, pHR was reconstituted into lipids (*26*) with a lipid/protein molar ratio of 30:1 using DMPC lipids (1,2 dimyristoyl phosphatidylcholine). The low lipid content guarantees a stable film on the ATR crystal after the buffer has been overlaid. The obtained reconstituted protein will be denoted as halorhodopsin membrane sheets. A similar lipid/protein ratio prevails in the bacteriorhodopsin purple membrane. DMPC Lipids were obtained from Sigma.

Preparation of NpHR Samples for Infrared Spectroscopy. For the attenuated total reflection (ATR) measurements, 30−40 μg (approximately 1.5 nmol) of NpHR membrane sheets were dried as a thin film onto the diamond ATR crystal. The protein was overlaid with a ~1 mL standard neutral pH buffer reservoir containing 200 mM MOPS (3-[*N*-morpholine]-propanesulfonic acid) at pH 7. The high buffer concentration minimizes unspecific effects on the membrane stack by varying the salt concentration.

For the time-resolved step−scan FTIR experiments so-called sandwich samples were used. This specially designed CaF_2 cuvette (*27*) provides a buffer reservoir of approximately 20 μL. This is important for the stabilization of blue NpHR and for controlling pH and ionic composition. Despite the large reservoir volume, only approximately 1.5 nMol of NpHR are needed, and the cuvette thickness is approximately 4 μm. Sample diameter is 5 mm. For the time-resolved FTIR study of blue NpHR, the solvent was 200 mM MOPS at pH 7.

Static ATR Measurements. ATR FTIR spectroscopy was performed with a Bruker IFS 28 spectrometer with a liquid nitrogen cooled MCT (mercury cadmium telluride) detector. A microdiamond ATR setup (SENSIR, 100 μm thickness, approximately 7 effective internal reflections) equipped with a temperature controller (25 °C) was used. IR spectra were recorded in blocks of 512 scans with a spectral resolution of 4 cm^{-1}. Film stability was checked by measuring the baseline. Anion titration measurements were performed by adding the required amount of the specific anion salt dissolved in 200 mM MOPS buffer at pH7 into the buffer reservoir up to the desired salt concentration.

Time-Resolved Infrared Measurements. The step−scan technique and its evaluation methods were described previously (*18*, *28*). Because we focused on the later intermediates of the blue NpHR photocycle, the slower detection system with an effective rise time of ∼600 ns was used. With this system, the signal from the detector preamplifier was further amplified (100- to 300-fold) with a commercial ac-coupled amplifier (DHPVA-200, FEMTO, Berlin). The sample was excited by the output of an OPO (Lambda Physik, Göttingen) tuned to 570 nm, which was pumped by the tripled output of an Nd:YAG laser (Brilliant, Quantel). Repetition rate was 5 Hz. Using neutral density filters, the pulse energy was reduced to ∼1.5 mJ at the sample position. In order to achieve a satisfactory signal-to-noise ratio, several measurements had to be averaged. Using between 8 and 16 flashes per sampling position of the interferometer, a total of 208 flashes per sampling were applied. Spectral resolution was 8 cm^{-1}. All step−scan measurements were performed at 20 °C.

RESULTS

Binding of Monoatomic Anions. In Figure 1a, the difference spectrum caused by the binding of Cl^- to blue NpHR is shown. The negative bands correspond to blue NpHR, whereas the positive bands reflect the anion-bound form. This state is called NphR576 according to its absorption maximum and corresponds to the dark state of the anion-transporting photocycle. We will use the light-induced difference spectra published before as a reference ((*18*) and Figures 1c and 6c−e). In agreement with these, the anion-binding spectrum is dominated by the ethylenic mode of the chromophore at 1525 cm^{-1} and by a fingerprint mode at 1207 cm^{-1} (the C14−C15 stretching mode). Also, other positive bands nicely reflect NpHR576, which will become clearer when we discuss the bands due to blue NpHR. The shoulder around 1632 cm^{-1} is partially caused by the C=N stretch of the protonated Schiff base because in the difference spectra of the photoycle, a rather large band at this position has been assigned to this mode in NpHR576. Its low intensity indicates

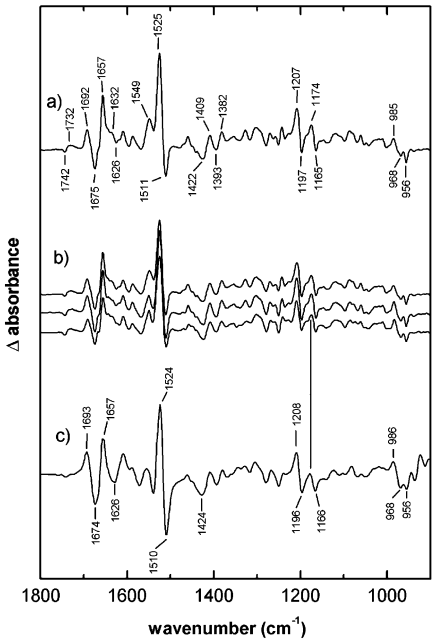

FIGURE 1: Comparison of static anion-binding spectra with the time-resolved spectra of the O intermediate. (a) Static chloride-binding spectrum, adding NaCl to a final concentration of 10 mM. (b) Comparison of chloride-, bromide-, and iodide-binding spectra (from the top). The final concentration of bromide and iodide was 10 mM. In the anion-binding experiments the buffer (MOPS at pH 7) concentration was kept constant at 200 mM. (c) Negative of the O intermediate spectrum taken from ref 18 (*18*). The spectra are normalized to each other using the size of the ethylenic difference band. Its size ranges from 1 to 3 mOD. Spectral resolution of the ATR measurements is 4 cm^{-1} and that of the spectrum of the O intermediate 8 cm^{-1}.

that a corresponding band of blue NpHR overlaps it. A similar observation has been made for the NpHR576 → O difference spectrum, and the corresponding band of O has also been assigned to the C=N stretch (see below). The other bands between 1700 and 1620 cm^{-1} can be probably assigned to amide I bands, indicating changes of the peptide backbone, induced by the anion binding. From the position of the difference band around 1740 cm^{-1}, it is tempting to assign it to an environmental change of Asp156. However, this would fix the corresponding band of NpHR576 around 1732 cm^{-1}, at least 7 cm^{-1} below the position deduced from the low-temperature and time-resolved NpHR576 → K difference spectra (*18*). Furthermore, the positive band in Figure 1a is much broader than what one would expect from the K difference spectra. Therefore, we have to assign it to a different carboxyl group, which we will discuss below.

The most prominent feature of blue pHR in Figure 1a is the negative band at 1511 cm^{-1}. It is assigned to the ethylenic stretching mode of the chromophore in blue NpHR. The negative bands at 1197 and 1165 cm^{-1} are assigned to fingerprint (C−C stretches coupled to CH in-plane bending) modes of the chromophore. There is a characteristic pattern of HOOP modes between 950 and 970 cm^{-1}, indicating that the chromophore is more twisted in the anion-depleted form (*29*). The negative band at 1742 cm^{-1} is more difficult to assign. One possibility could be that it represents the counterpart of the positive band at 1732 cm^{-1} described above, indicating an environmental change of this carboxyl group. However, the spectrum reflecting nitrate binding provides evidence that the features observed here are best

described by a rather narrow difference band (1742−/1736+) which might be assigned to Asp156 and an additional carboxyl group causing the broad positive band centered around 1728 cm^{-1}. The latter band would represent a protonation step concomitant with the anion binding. The superposition of this positive band and the positive part of the difference band results in the positive feature at 1732 cm^{-1} (see below).

In Figure 1b, the spectra reflecting the binding of the monoatomic anions Cl^-, Br^-, and I^- to blue NpHR are shown. In order to correct for small variations in the amount of protein and differences in the dissociation constant (1 mM for Br^-, 2.5 mM for Cl^-, 3 mM for I^- (*17*, *19*)), the spectra are normalized to each other, using the most prominent bands as standards. It is evident that the spectra are very similar. Obviously, the size of the anion (1.81 Å Cl^-, 1.91 Å Br^-, and 2.2 Å I^-) hardly influence the spectra. Therefore, they are induced by the change of the electrostatics in the neighborhood of the Schiff base rather than by changes of steric interactions.

Many models of the anion-translocating photocycle assume that the O state represents an anion-free protein conformation. Therefore, in Figure 1c, we compare the O → NpHR576 difference spectrum published earlier (*18*) with the chloride-binding spectrum of Figure 1a. It is obvious that they are very similar, which clearly shows that the O intermediate can be essentially identified with blue NpHR. It follows that the O decay just reflects the rebinding of the anion. Also, the HOOP modes between 950 and 970 cm^{-1} can be seen. Thus, the HOOP mode in O is not a consequence of photoisomerization but is due to structural changes induced by anion release. The identification of O with the static ion-depleted form is also supported by our observation that the decay of O is considerably slowed down at low chloride concentration. With our sample preparation (Materials and Methods), we are now able to better control the composition of the solvent, in contrast to the film samples used earlier (*18*). We observe an increase from 10.5 ms to more than 100 ms by reducing the chloride concentration from 100 to 3 mM (data not shown). For the latter, we had to take into account the fact that a considerable amount of anion-free blue NpHR is present in the dark, and therefore, this photocycle had to be included in the evaluation of the kinetic constants. However, because it is considerably faster (see below), it does not interfere with the much slower decay of essentially O to the NpHR576-blue NpHR equilibrium (or NpHR576-O equilibrium). The value of 10.5 ms is in reasonable agreement with the anion-binding data of stopped-flow measurements with blue NpHR (*30*), but it is somewhat slower than the O decay reported from UV−vis measurements of the photocycle (*21*). It is surprising that the C=N stretch of O and NpHR576 are similar because our data have clearly shown that the anion is released, and thus, the Schiff base region must be altered.

A small deviation from the O → NpHR576 spectrum is visible in the anion-uptake spectrum. In all three spectra of Figure 1c, there is a clear positive band at 1174 cm^{-1}, which is missing in the O → NpHR576 spectrum. This band belongs to the so-called fingerprint region in which the C−C stretching modes coupled to the CH bending modes show up. These bands are characteristic of the chromophore configuration. In both states of the O → NpHR576 difference spectrum, the chromophore is all-trans, despite the fact that the chromophore composition of the dark state of pHR is 85% trans and 15% cis, irrespective of the preillumination condition (*3*). Apparently, only the part containing the all-trans chromophore contributes to the photocycle (*31*). Even if the chromophore composition in blue pHR has not been determined, it is evident that at least in the anion-bound state the 13-cis chromophore must contribute to the anion-uptake difference spectra, and the positive band at 1174 cm^{-1} would correspondingly be caused by the fingerprint mode of the 13-cis form. Using pre-resonance Raman spectroscopy, the main fingerprint band of the 13-cis form of HsHR has been assigned to a band at 1183 cm^{-1}, and the same band position has been inferred for the corresponding band of NpHR (*3*). Thus, the 1174 cm^{-1} band cannot be directly identified with this mode. However, one has to take into consideration that a corresponding negative band, that is, the fingerprint mode of the 13-cis form of blue NpHR is also present. Because, as the spectra demonstrate, the removal of the anion considerably alters the fingerprint modes, it is difficult to predict the fingerprint modes of the 13-cis form of blue NpHR. Thus, we tentatively assign the feature around 1174 cm^{-1} to the overlap of the main fingerprint band of the 13-cis form of NpHR with a corresponding band of the anion-free form.

Binding of Nitrate and Azide. NpHR also pumps nitrate with the same efficiency as the monoatomic anions (*2*). The dissociation constant has been determined to be 16 mM (*19*). This is surprising in view of the different shape of nitrate compared to that of the other anions, suggesting that the interaction with the protein also exhibits special features not present in the binding spectra of the monoatomic anions. Azide has been reported to cause proton pumping in the direction as found for bacteriorhodopsin, and it has been concluded that the bound azide functions as the primary proton acceptor for Schiff base deprotonation (*32*). Thus, azide is not transported. The geometry of azide is linear and, again, differs considerably from that of the other anions. The dissociation constant of 33 mM (*19*) indicates only weak binding. Because of these properties, one would expect the binding spectra of nitrate and azide to differ considerably from those of the monoatomic anions.

Nitrate has IR absorption bands between 1300 and 1420 cm^{-1}, depending on the environment. Therefore, one has to correct the binding spectra caused by the addition of nitrate for the bands of nitrate in solution. The spectra can be compared with those of the monoatomic anions only after appropriate corrections have been made. This correction is known for ATR spectroscopy as the excluded volume correction, that is, the volume excluded by the membrane. This correction is not straightforward because, as the absorption spectra of the NpHR sheets on the ATR plate have shown, considerable swelling occurs upon addition of the buffer. Therefore, we adopted an intrinsic correction method that does not rely on the determination of the excluded volume.

Because the specific anion binding site can be saturated at relatively low nitrate concentrations (dissociation constant of 16 mM), the difference spectrum obtained by increasing the nitrate from 70 to 90 mM shows small changes caused by the binding of nitrate to residual blue halorhodopsin but large bands due to the increase of the aqueous nitrate

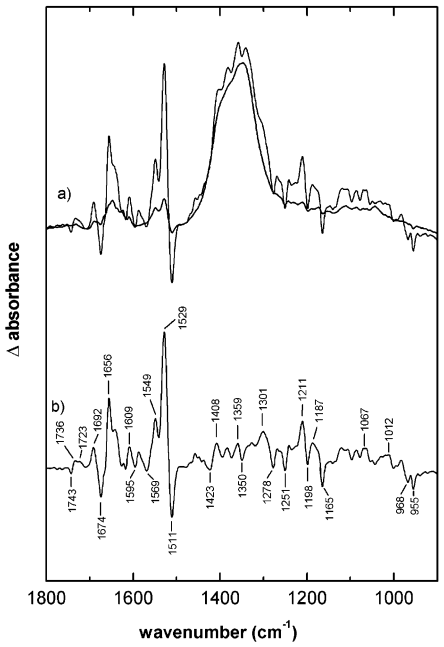

FIGURE 2: Nitrate-binding spectra. (a, black) Spectrum obtained by raising the nitrate concentration from 0 to 20 mM; (a, gray) Spectrum obtained by raising the concentration from 70 to 90 mM. (b) Difference of the two spectra in a. The buffer (MOPS at pH 7) concentration was kept constant at 200 mM. Spectral resolution is 4 cm^{-1}.

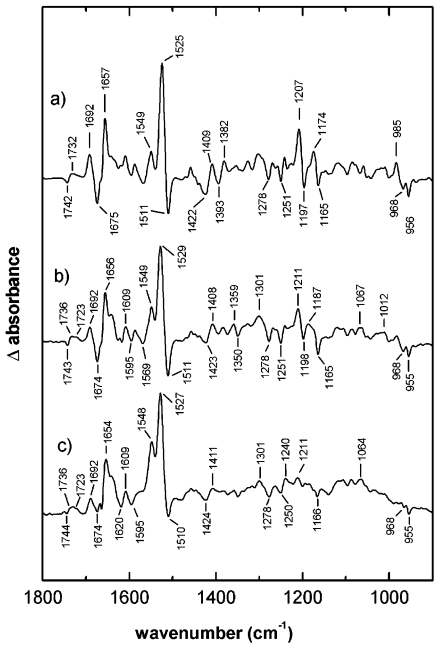

FIGURE 3: Comparison of chloride- (a), nitrate- (b), and (c) azide-binding spectra. Spectrum a is from Figure 1a and b from Figure 2b. In c, the azide concentration was 10 mM. As before, the MOPS buffer (at pH 7) concentration was kept constant at 200 mM. Spectral resolution is 4 cm^{-1}.

concentration by 20 mM. However, in the difference spectrum obtained by increasing the nitrate concentration from 0 to 20 mM, large bands due to nitrate binding to blue NpHR show up accompanied, as before, by large bands due to nitrate in solution at the same concentration of 20 mM. Both difference spectra were obtained with the same sample, starting from 0 mM nitrate and subsequently increasing the concentration to 20, then to 70, and finally to 90 mM. Therefore, the two difference spectra can be directly subtracted, thereby correcting the first spectrum for the aqueous nitrate. The bands due to nitrate binding to blue NpHR are uniformly somewhat reduced. This procedure is shown in Figure 2. The two spectra in Figure 2a show the binding spectra obtained by increasing the nitrate concentration from 0 to 20 mM (black) and from 70 to 90 mM (gray). Figure 2b shows the difference between the two spectra.

Azide does not cause similar problems. It has a strong band at 2048 cm^{-1} in H_2O, caused by the antisymmetric stretching mode, which is outside the spectral range discussed here. The symmetric stretching mode has its frequency around 1337 cm^{-1}. However, control measurements showed that its intensity is so small that it can be neglected. We were, however, faced by another difficulty. Azide causes the shrinking of the membrane stack on the ATR crystal, causing distortions of the binding-induced difference spectrum by the absorption feature of the denser membrane stack, as can be seen especially by the broad absorbance increase in the amide I/II region. Therefore, we could only evaluate the binding up to 10 mM, inducing correspondingly small bands (the dissociation constant is 33 mM (*19*)). But even so, the shrinking can still be seen at this low concentration, causing a shift of the bands in the difference spectrum toward positive absorbance changes, especially in the amide I/II spectral range (Figure 3c).

In Figure 3, we compare the spectrum obtained by chloride binding with the nitrate- and azide-binding spectra, the latter two obtained as described above. It is obvious that the chloride- and nitrate-binding spectra are generally very similar, although subtle differences are present. In the fingerprint region here, the nitrate-binding spectrum resembles the O → NpHR576 spectrum shown in Figure 1c, that is, the positive band at 1174 cm^{-1} is clearly missing. Thus, if the interpretation of this band given above is correct, we would have to conclude that nitrate binds only to the all-trans form. We admit that this interpretation is not unequivocal. But we emphasize that the exact interpretation does not influence the main conclusions deduced from chloride- and nitrate-binding spectra.

Further differences can be seen between 1300 and 1400 cm^{-1}. Because the bands of nitrate also show up in this spectral range, it is tempting to assign these features to bands of bound nitrate. However, below, we demonstrate using isotopic labeling of nitrate that these features are considerably larger than the bands due to nitrate bound to pHR. As expected from the absorption maxima λ_{max}, the ethylenic stretching mode differs somewhat for the Cl^- and nitrate-bound species (576 nm and 1525 cm^{-1}, 569 nm and 1529 cm^{-1}, respectively (*33*, *34*)). It appears that the features ascribed to protonated carboxyl groups are also slightly altered. Whereas in the chloride-bound state a single broad positive band arises at 1732 cm^{-1}, in the nitrate-bound form, the positive band is clearly split (1736 and 1723 cm^{-1}), supporting the assignment of the spectral features to two carboxyl groups, one, Asp156, undergoing an environmental change, the other becoming protonated, as suggested above. In the Discussion section, we will suggest a possible group. In the case of the monatomic anions, the position of the band caused by protonation is closer to the difference band, making it more difficult to separate the two bands.

The feature between 1720 and 1745 cm^{-1} (Figure 1c) is not observed in the spectrum of the O itermediate (Figure 1d). Only a very small negative band at 1742 cm^{-1} could indicate deprotonation of a carboxyl group in the transition to the dark state, and we will suggest a group later. At present, we do not have a clear-cut explanation for this difference between the spectrum of the O and the static anion-binding spectra. One has to consider that O is a transient species, decaying within several ms, whereas blue NpHR is a stable species, and the titration experiments run over more than 10 min. Thus, it could be that the molecular changes causing the features around 1735 cm^{-1} need some time to develop.

Surprisingly, the azide-binding spectrum is, within the uncertainties caused by the difficulties in generating the spectrum, also very similar to the chloride-binding spectrum. The small deviations described for the nitrate-binding spectrum seem to pertain here as well. It appears that the deviation of the anion shape from a sphere and the corresponding charge distribution cause some small but distinct structural alterations. In the spectral range between 1300 and 1400 cm^{-1}, where additional differences are observed for nitrate and azide binding, CH bending modes of aliphatic parts of amino acid side chains and the COH modes of serine would be expected (*35*). Interestingly, the interaction of the anion with HsHR involves such groups (especially CH_3 of Thr111 and COH of Ser115) (*1*).

So far, we have not identified the bands caused by bound nitrate. The NO stretching vibrations (spectral region between 1300 and 1500 cm^{-1}) are influenced by the mode of binding (*36*, *37*). They could, therefore, provide information on the binding pocket. However, the great binding similarity of the chloride- and nitrate-binding spectra (Figure 3) shows that the bands caused by bound nitrate must be small. Therefore, we measured a nitrate-binding spectrum with ^{15}N-nitrate in the same way as that demonstrated in Figure 2 and compared it with the spectrum obtained with unlabeled nitrate. The results are shown in Figure 4. It is evident that the deviations observed in the nitrate-binding spectrum around 1400 cm^{-1} mentioned above are also present in the spectrum with labeled nitrate (Figure 4d). Thus, this feature reflects bands of protein groups that are altered by the considerably differing shape and chemistry of the nitrate anion. The effect on the protein causes larger bands than the bound nitrate itself (Figure 4d). Therefore, from the comparison of the two spectra in Figure 4d, the bands of bound nitrate cannot be directly identified. We subtracted the two spectra, using the large chromophore bands for normalization. The result is shown in Figure 4e, the spectrum being multiplied by a factor of 2. The subtraction is not perfect. The broadband around 1050 cm^{-1} is caused by baseline distortion present in the spectrum containing labeled nitrate, as control measurements have shown. Furthermore, there is increased noise in the amide I region because of the low transmission of the sample, and the large band due to the C═C difference band cannot be completely compensated. Despite these deficiencies, the label effect of bound nitrate can be clearly seen. The negative features at 1432 and 1405 cm^{-1} are caused by the unlabeled nitrate, and the positive ones at 1383 and 1371 cm^{-1} represent the labeled nitrate. Because of the small size of the bands, one has to discuss the reliability of this assigment. The measurements have been repeated three times, and the general features were always reproduced. However, we cannot exclude the fact that the difference only reflects a broad negative and positive band, the fine structures being caused by noise. We will discuss both cases below.

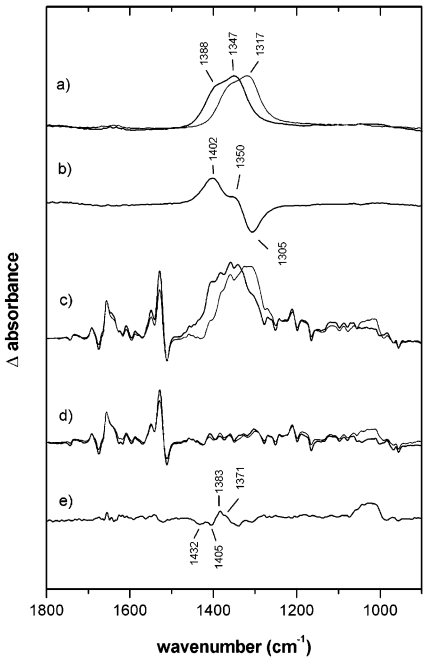

FIGURE 4: Identification of bands caused by bound nitrate. (a) Spectra of 12.5 mM labeled (gray) and unlabeled (black) nitrate in aqueous buffer. (b) Difference of the two spectra, unlabeled minus labeled. (c) Spectra obtained by adding 20 mM nitrate to the sample, labeled (gray) and unlabeled (black). (d) Pure nitrate-binding spectra obtained from the spectra shown in 4c, as described in the text, labeled (gray) and unlabeled (black) nitrate. (e) Difference of the two spectra from Figure 4d, labeled minus unlabeled, using the chromophore bands for normalization. The buffer concentration for all spectra was kept at 200 mM MOPS at pH 7. Spectral resolution is 4 cm^{-1}.

It is well documented that the splitting of the NO stretching modes of nitrate strongly depends on the interaction with the environment. In a completely isotropic medium (D_{3h} symmetry) , the two NO stretching modes are degenerate, and therefore, only one band shows up. The spectrum of nitrate in aqueous solutions clearly shows the splitting (Figure 4a), indicating that the hydrogen bonding of water molecules renders the 3 NO bonds nonequivalent even on the time scale of vibrational relaxation, that is, around 10 ps. Thus, the molecule experiences an effective C_{2v} symmetry. However, the splitting of ~40 cm^{-1} is considerably less than that observed for $Ca(NO_3)_2$ (90 cm^{-1} (*38*)).

The nitrate bands in Figure 4e could only be deduced by forming the double difference spectrum between the two binding spectra with labeled and nonlabeled nitrate, and the question arises as to what extent the subtraction impairs the identification of the splitting. As the subtraction of the spectra of aqueous unlabeled and labeled nitrate shows, negative and positive bands partially superimpose (Figure 4b). Therefore, the splitting in aqueous nitrate cannot be directly determined in the subtraction because it is of a size similar to that of the isotopic shift. However, if the splitting is smaller than the isotopic shift, it can be resolved in the double difference spectrum.

If we take the fine structure in the double difference to be real, then the splitting (27 cm^{-1}) of protein bound nitrate

would be considerably less than that observed for nitrate in H_2O (41 cm^{-1}). If the fine structure is taken as noise, then the center of the positive and negative bands are separated by 35 cm^{-1}, as expected for the isotopic shift. This would indicate a splitting even smaller than 27 cm^{-1}. Thus, in any case, the considerably smaller splitting observed for nitrate bound to NpHR compared to that of nitrate in H_2O shows that the influence of the binding site on the nitrate is more isotropic.

In addition to the splitting, an estimate of the extinction coefficient also provides useful molecular information on the binding site, and a binding site considerably deviating from an aqueous environment is supported. Figure 4c and e show that the bands due to nitrate bound to pHR in the ATR experiment are considerably smaller than those of nitrate dissolved in the intercalating buffer. For an evaluation, one has to make an estimate of the halorhodopsin concentration in the membrane. Taking an area of 35 nm^2 for a BR trimer in the purple membrane and a thickness of 5 nm, one determines the volume of the trimer to be 175 nm^3, resulting in a concentration of about 28 mM. Furthermore, an estimate of the excluded volume is needed. For this, one has to take into account the fact that the stack of membranes on the ATR plate is thicker than the penetration depth of the IR beam (1 μm). If one regards the stack of membranes as alternating layers of membranes of thickness d_1 and the nitrate-containing buffer of thickness d_2, the excluded volume is proportional to d_1. Because the bands of aqueous nitrate and nitrate bound to NpHR are quite different, the excluded volume can be estimated from spectra a and c of Figure 4. The ratio of the absorbance of aqueous nitrate (arbitrary units) divided by the concentration (12.5 mM) in Figure 4a is approximately 0.6, whereas it is 0.5 for the concentration of 20 mM in Figure 4c. Thus, the excluded volume is approximately 20%, that is, 20% are occupied by NpHR-containing membranes. From the data shown in Figure 4, we can now compare the extinction coefficients. The double difference labeled minus unlabeled (Figure 4e) shows that the absorbance due to bound nitrate is only 5% of that of the aqueous nitrate of Figure 4c. This factor is called *k*. Because the halorhodopsin concentration in the membrane is 28 mM (c_1) and the aqueous nitrate concentration is 20 mM (c_2), the extinction coefficient of bound nitrate is calculated as follows.

$$\epsilon_{bound} = c_2/c_1 \cdot k \cdot \epsilon_{aq} \cdot d_2/d_1 = 0.14 \cdot \epsilon_{aq}$$

where ϵ_{bound} is the extinction coefficient of bound nitrate and ϵ_{aq} that of aqueous nitrate. Thus, even if we allow in this calculation for some overestimation of the halorhodopsin concentration in the membrane (50%) and for some overestimation of the excluded volume (20%), we can conclude that the extinction coefficient of nitrate bound to NpHR is considerably smaller than that of aqueous nitrate. This is probably caused by the reduced polarity of the binding site, which is also discussed in the evaluation of the structure of HsHR (*1*).

Photocycle of Blue NpHR. As we have shown, the anion release and rebinding during the active photocycle causes larger amide I bands and, therefore, larger backbone changes than the light-induced isomerization of the chromophore itself (*18*). It has been shown that blue NpHR also undergoes a photocycle (*19*) without anion translocation, which presumably involves an all-trans → 13-cis isomerization. Therefore, it is interesting to compare the isomerization-induced conformational changes in these two photocycles. For this purpose, we have investigated the photocycle of blue NpHR by time-resolved step−scan FTIR spectroscopy. Time-resolved UV−vis measurements with 10 μs time-resolution have identified a blue-shifted intermediate that relaxes back to the dark state (*19*). The time-resolved FTIR results are shown in Figure 5. Here, we have fitted the time-resolved difference spectra to a sum of exponentials yielding the amplitude spectra, and from these spectra, the intermediate spectra have been derived assuming an unidirectional reaction model. These procedures have been described previously (*18*, *28*). A reasonable fit was obtained with two exponentials with half times of 2.5 and 460 μs. Thus, two intermediates can be identified. In Figure 5a and b, the two amplitude spectra are shown, and in Figure 5c and d the two spectra of the intermediates are shown. The photocycle is considerably shortened by approximately a factor of 10, in agreement with the UV−vis measurements (*19*). In the first intermediate spectrum (Figure 5c), there is a strong HOOP mode at 979 cm^{-1}, characteristic for early intermediates of the photoreaction of bacterial rhodopsins. A comparison with spectra of BR (*28*), NpHR (*18*) and pharaonis sensory rhodopsin II (*39*, *40*) suggests that it is the 15-HOOP mode. If this is correct, it would indicate that the chromophore is strongly twisted around the retinal $C_{14}-C_{15}$ single bond, adjacent to the Schiff base (*29*). The band pattern between 1100 and 1220 cm^{-1}, the finger print region of the chromophore, clearly shows that the all-trans → 13-cis isomerization has already occurred in this intermediate. The interpretation of the region between 1490 and 1560 cm^{-1} is less straightforward. Here, the amide II changes and the ethylenic modes of the retinal also contribute. If the latter can be identified, the absorption maximum of the intermediate can be deter-

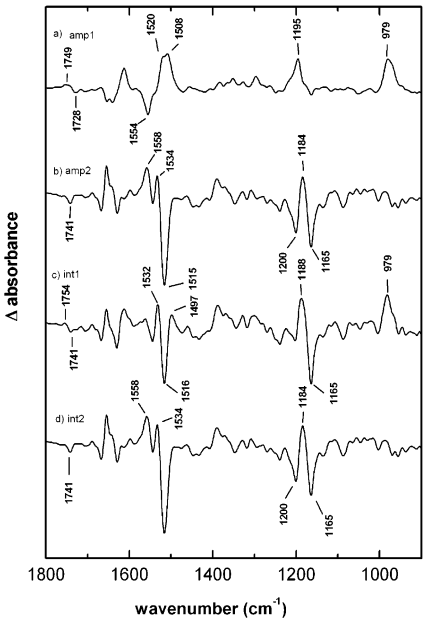

FIGURE 5: Amplitude and intermediate spectra of the global fit of the time-resolved step−scan FTIR spectra of blue NpHR. (a) First amplitude spectrum with a half-time of 2.5 μs. (b) Second amplitude spectrum with a half-time of 460 μs. (c) First intermediate spectrum. (d) Second intermediate spectrum. Spectral resolution is 8 cm^{-1}, and the temperature was 20 °C.

mined (*33*, *34*). The negative band at 1516 cm^{-1} is close to the negative band of the anion titration experiments. Taking the different overlap of positive and negative bands into account as well as the poorer spectral resolution in the time-resolved spectra, the negative band can be identified with the ethylenic mode of blue NpHR. There are two positive bands at 1532 and at 1497 cm^{-1}. The former would indicate a blue-shifted intermediate, whereas the latter a red-shifted one. Some more information can be obtained from the first amplitude spectrum, essentially representing the decay of the first intermediate to the next one. The corresponding positive band in this spectral range is broad and split (1520 and 1508 cm^{-1}). Because it is a common feature of the first intermediate of retinal proteins exhibiting a strong HOOP mode to be red-shifted, we assign the band at 1508 cm^{-1} to the ethylenic mode of the first intermediate; the other band probably corresponds to amide II changes. A corresponding negative band is located at 1554 cm^{-1}, also corresponding to amide II changes. (For ethylenic mode of the second intermediate, the frequency is too high because it would correspond to a strongly blue-shifted species with an absorption maximum around 480 nm, in contradiction to the time-resolved UV−vis measurements by which an absorption maximum of 550 nm had been determined.) Therefore, we have to conclude that we cannot identify the ethylenic mode of the second intermediate. A possible explanation is obtained from the intermediate spectra. In both spectra, a positive band is observed around 1532 cm^{-1}. In the first intermediate spectrum, it would be assigned to an amide II band, whereas in the second intermediate having a λ_{max} of 550 nm, it would correspond to the ethylenic mode (*33*, *34*). We admit that other interpretations may be possible. Without isotopic labeling of the chromophore, an unequivocal decision cannot be made. However, the interpretation does not influence our main conclusions when we compare the difference spectra of blue NpHR with those of the NpHR576. Concomitant with the amide II changes between the two intermediates, there are changes in the amide I range between 1620 and 1680 cm^{-1}.

The feature around 1740 cm^{-1} deserves special attention. The position suggests that it is due to Asp156. The difference band in the first intermediate spectrum indicates that it is upshifted, and the negative band in the second intermediate spectrum suggests that it deprotonates. This result is quite challenging because this aspartic acid (and the corresponding residue, Asp115, in bacteriorhodopsin) have been regarded as essentially inert against protonation changes. If one compares blue NpHR with blue BR, we expect that Asp256 is deprotonated as Asp212 in blue BR. Therefore, it cannot explain the negative band at 1741 cm^{-1}. Furthermore, the additional carboxyl group, which becomes protonated during anion binding, cannot explain this band because it is also deprotonated in blue NpHR. In the Discussion section, we will propose an alternative to Asp156.

DISCUSSION

The anion-binding spectra obtained with static ATR FTIR spectroscopy convincingly demonstrate that the decay of O simply reflects the passive uptake of the anion. During this process, the chromophore relaxes into a more planar conformation. It is important to emphasize that this relaxation is independent of the type of anion as long as it occupies the binding site. Thus, some part of the binding energy might derive from the energy stored in the distorted chromophore. Despite the range of dissociation constants from 1 to 33 mM, the binding spectra for the different anions are very similar and for the monoatomic anions, almost identical. The specificity of the binding must, therefore, be caused by more subtle differences in the interaction of the anions with the binding site. In addition, changes in the hydration shell have to be taken into account. The crystal structure of HsHR reveals one OH group from serine 115, the CH_3 group from threonine 111, the Schiff base proton, and two coordinated water molecules interacting with the chloride. However, although the same residues are also present in NpHR, the dissociation constant of chloride in NpHR (3 mM) is lower at least by 1 order of magnitude than that in HsHR. A dissociation constant of 80 mM for HsHR has been deduced from photocycle measurements (*41*), which is not too far from the 50 mM value obtained by transport activity measurements of cell envelope vesicles (*42*) and the 100 mM value obtained from electrical measurements (*14*). Only in electrical measurements of HsHR attached to a black lipid film has a dissociation constant of 7 mM been deduced (*43*). Surprisingly, despite the higher affinity for chloride, NpHR pumps nitrate as well as chloride, in contrast to HsHR (*2*). Thus, care must be taken in comparing the anion binding sites of the two systems. From the titration experiments, we do not find evidence for the presence of an additional binding site with higher affinity, in agreement with UV−vis absorption and CD measurements (*11*, *19*) but in contrast to UV−vis absorption measurements by another laboratory (*12*). Interestingly, the crystal structure of HsHR also shows only one bound chloride.

We have identified two carboxyl groups that undergo protonation changes. One group becoming protonated with anion uptake and another group showing up in the photocycle of blue NpHR, which becomes deprotonated with the formation of the second intermediate. Thus, these two groups must be different.

With respect to the first group, it is interesting to note that in the D85S mutant of BR, chloride binding is accompanied by proton uptake, and the proton acceptor has been identified with Glu204 (*44*). In NpHR, there is no caboxyl group at this position; however, Glu234, the homolog of Glu194 in BR, is present. Because in BR Glu194 and Glu204 are in close proximity, it is reasonable to assume that in NpHR Glu234 becomes protonated upon anion binding.

The identification of the group showing up in the photocycle of blue NpHR is less clear. As already mentioned, Asp252 can be excluded, and Asp156 is highly unlikely. It should also be mentioned that in the O intermediate, a small positive band can be seen at this position. Thus, we have to search for another carboxyl group. One possibility could be that, as in HsHR, a palmitic acid is bound. As the structure of HsHR shows, the carboxyl group makes a hydrogen bond with the OH group of Thr111 (*1*). Thus, it might well be that it reacts on anion release and on the photoreaction in blue NpHR. Because the band position is close to that presumed for Asp156, some assignments to this residue should be reconsidered. In order to clarify this point, experiments with labeled palmitic acid are in progress.

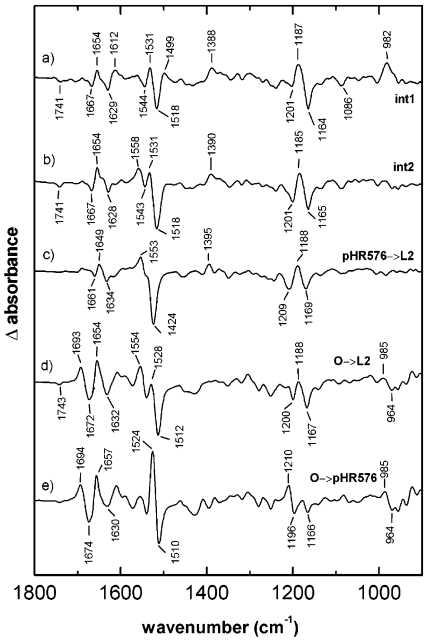

FIGURE 6: Comparison of the time-resolved spectra of the photocycles of pHR576 and blue NpHR. (a) Spectrum c of Figure 5. (b) Spectrum d of Figure 5. (c) L2 intermediate spectrum of NpHR576. (d) Amplitude spectrum of the L2 → O transition. (e) Negative of the O intermediate spectrum. The last three spectra are taken from Hackmann et al. (*18*). Spectral resolution is 8 cm^{-1}.

Binding of the monoatomic anions bromide, chloride, and iodide causes, within our spectral accuracy, the same difference spectra, even in the spectral range where the arginine side chain (Arg123, 1620−1680 cm^{-1}, deprotonated Asp252 (1560−1600 and 1360−1420 cm^{-1}) and the COH group of Ser130 (1050−1420 cm^{-1}) absorb (*35*). Therefore, the same structural changes are induced. But even the binding of nitrate and azide causes very similar difference spectra, small deviations in the spectral range between 1300 and 1400 cm^{-1} possibly caused by aliphatic CH groups and the COH group of Ser130. The small or possibly even absent splitting of the bands of bound nitrate and the considerably reduced absorption strength indicate, compared to those of the aqueous solvent, a more isotropic and less polar binding site.

In Figure 6, we compare several spectra of the native photocycle (*18*) with the intermediate spectra of the photocycle of blue pHR. The purpose is to compare the molecular changes of the protein as indicated by amide I changes induced by chromophore isomerization or by anion uptake and release. The first two spectra (6a and b) are the intermediate spectra of blue pHR reproduced from Figure 5. The next spectrum, 6c, is the difference spectrum of the L2 intermediate in the physiological photocycle with chloride as anion. Spectrum 6d is the amplitude spectrum obtained from the global fit describing the L2 → O transition, that is, the anion release, and the last spectrum represents the negative of the O intermediate spectrum, that is, the difference spectrum between O and NpHR576. As we have shown by the titration experiments, this spectrum is equivalent to the binding of the anion to blue NpHR. The last three spectra have been published (*18*). It is obvious that the L2 difference spectrum (anion-transporting photocycle) and the spectrum of the second intermediate of the photoreaction of blue pHR (transport inactive photocycle) are qualitatively similar, the main difference being the positive band at 1531 cm^{-1} in the latter, which we have assigned to the ethylenic mode of the chromophore in this intermediate. Because the absorption maximum of L2 is around 520 nm (*17*), the corresponding ethylenic mode is expected to be around 1550 cm^{-1}, which has been confirmed by resonance Raman experiments. We have concluded before that the intensity of this band must be very low and that it is hidden under the larger amide II changes (*18*).

Both the anion release and the anion uptake spectra exhibit the largest amide I changes. In the way the two spectra are presented in Figure 6d and e, the negative bands are caused by blue NpHR (respectively the O intermediate). However, in the release spectrum, the positive bands belong to L2 with a 13-cis chromophore, whereas in the uptake spectrum, the positive bands are cause by NpHR576 with an all-trans chromophore. Thus, the release/uptake of the anion causes the largest protein distortions and the chromophore isomerization considerably smaller ones. We conclude from the titration spectra that the distortion of the protein induced by the release of the anion even causes distortion of the chromophore because the HOOP mode shows that the chromophore is twisted.

Compared to the proton in the much better understood proton pump bacteriorhodopsin, the transported ions in halorhodopsin are sterically more demanding (*1*). However, because the binding spectra depend very little on the shape and size of the anions, the negative charge of the anion within the protein probably exerts a larger effect. In agreement with time-resolved UV−vis measurements (*17*), we have concluded from our time-resolved FTIR studies (*18*) that the dissociation constant of the release site is larger than 4 M in the O intermediate. Although we have identified the conformational changes for the O state, mechanistically, there must be a state with similar conformation to which the anion is still bound. Such a state can be stabilized at high chloride concentration, and we have concluded that this leads to a photocycle without anion transport (*18*). The dissociation constant for the anion uptake has also been deduced to be high in O (approximately 1 M (*17*)). However, because it is low in NpHR576, the anion uptake finally takes place even at rather low anion concentrations. A dissociation constant larger than 4 M probably represents a conformation with an opening toward the cytoplasmic anion channel. Our results presented here and our previous time-resolved FTIR studies are also in agreement with the suggestion that the transfer of the anion from a region still close to the Schiff base in L2 to the release site represents a diffusion-like process (*11*) that has the largest electrogenicity (*22*). It has been suggested that in L2 the anion is close to Thr218 and a water molecule (*11*). The corresponding channel, which is according to the structure of HsHR blocked in the dark state, probably opens up in the intermediate state with an O conformation, allowing some water molecules to penetrate and provide the solvation of the anion and its release to the cytoplasm. Another consequence of the conformational changes could be the increase of the dissociation constant of the uptake site to around 1 M. With the binding of the anion to the uptake site close to the Schiff base via a bimolecular reaction, the conformational changes are reverted, the cytoplasmic channel is closed, and the high-affinity uptake site is restored. In the photoreaction of blue NpHR, the backisomerization occurs within 600 μs. Thus, the backisomerization of the chro-

mophore in the anion-translocating photocycle is probably not the rate-limiting step but the formation of the conformational changes leading to the open conformation and anion release. They manifest in the larger amide I bands. The role of retinal isomerization is, therefore, 2-fold. First, it moves the anion from the uptake site to the site in L2. Second, it causes conformational changes of the protein in order to allow the release of the anion even under high salt concentration. A similar protein conformation can otherwise be produced only in blue NpHR by low anion concentration.

ACKNOWLEDGMENT

We thank A.A. Wegener for preparing NpHR and R. Vogel for critical comments.

REFERENCES

1. Kolbe, M., Besir, H., Essen, L. O., and Oesterhelt, D. (2000) Structure of the light-driven chloride pump halorhodopsin at 1.8 Å resolution, *Science 288*, 1390−1396.
2. Duschl, A., Lanyi, J. K., and Zimányi, L. (1990) Properties and photochemistry of a halorhodopsin from the haloalkaliphile, *Natronobacterium pharaonis*, *J. Biol. Chem. 265*, 1261−1267.
3. Zimányi, L., and Lanyi, J. K. (1997) Fourier transform Raman study of retinal isomeric composition and equilibration in halorhodopsin, *J. Phys. Chem. B 101*, 1930−1933.
4. Sasaki, J., Brown, L. S., Chon, Y.-S., Kandori, H., Maeda, A., Needleman, R., and Lanyi, J. K. (1995) Conversion of bacteriorhodopsin into a chloride ion pump, *Science 269*, 73−75.
5. Tittor, J., Haupts, U., Haupts, C., Oesterhelt, D., Becker, A., and Bamberg, E. (1997) Chloride and proton transport in bacteriorhodopsin mutant D85T: different modes of ion translocation in a retinal protein, *J. Mol. Biol. 271*, 405−416.
6. Paula, S., Tittor, J., and Oesterhelt, D. (2001) Roles of cytoplasmic arginine and threonine in chloride transport by the bacteriorhodopsin mutant D85T, *Biophys. J. 80*, 2386−2395.
7. Lanyi, J. K., Duschl, A., Váró, G., and Zimányi, L. (1990) Anion binding to the chloride pump, halorhodopsin, and its implications for the transport mechanism, *FEBS Lett. 265*, 1−6.
8. Maeda, A., Ogurusu, T., Yoshizawa, T., and Kitagawa, T. (1985) Resonance raman study on binding of chloride to the chromophore of halorhodopsin, *Biochemistry 24*, 2517−2521.
9. Pande, C., Lanyi, J. K., and Callender, R. H. (1989) Effects of various anions on the Raman spectrum of halorhodopsin, *Biophys. J. 55*, 425−431.
10. Sato, M., Kikukawa, T., Araiso, T., Okita, H., Shimono, K., Kamo, N., Demura, M., and Nitta, K. (2003) Ser-130 of *Natronobacterium pharaonis* halorhodopsin is important for the chloride binding, *Bioph. Chem. 104*, 209−216.
11. Sato, M., Kubo, M., Aizawa, T., Kamo, N., Kikukawa, T., Nitta, K., and Demura, M. (2005) Role of putative anion-binding sites in cytoplasmic and extracellular channels of *Natromonas pharaonis* halorhodopsin, *Biochemistry 44*, 4775−4784.
12. Kalaidzidis, I. V., and Kalaidzidis, Y. L. (2003) Occupancy of two primary chloride-binding sites in *Natronobacterium pharaonis* halorhodopsin is a necessary condition for active anion transport, *Biochemistry (Moscow) 68*, 354−358.
13. Koyama, K., Sumi, M., Kamo, N., and Lanyi, J. K. (1998) Photoelectric response of halorhodopsin from *Natronobacterium pharaonis*, *Bioelectrochem. Bioenerg. 46*, 289−292.
14. Okuno, D., Asaumi, M., and Muneyuki, E. (1999) Chloride concentration dependency of the electrogenic activity of halorhodopsin, *Biochemistry 38*, 5422−5429.
15. Muneyuki, E., Shibazaki, C., Wada, Y., Yakushizin, M., and Ohtani, H. (2002) Cl^- concentration dependence of photovoltage generation by halorhodopsin from *Halobacterium salinarum*, *Biophys. J. 83*, 1749−1759.
16. Rüdiger, M., and Oesterhelt, D. (1997) Specific arginine and threonine residues control anion binding and transport in the light-driven chloride pump halorhodopsin, *EMBO J. 18*, 3813−3821.
17. Chizhov, I., and Engelhard, M. (2001) Temperature and halide dependence of the photocycle of halorhodopsin from *Natronobacterium pharaonis*, *Biophys. J. 81*, 1600−1612.
18. Hackmann, C., Guijarro, J., Chizhov, I., Engelhard, M., Rödig, C., and Siebert, F. (2001) Static and time-resolved step-scan FTIR investigations of the photoreaction of halorhodopsin from *Natronobacterium pharaonis*: Consequences for the anion translocation mechanism, *Biophys. J. 81*, 394−406.
19. Scharf, B., and Engelhard, M. (1994) Blue halorhodopsin from *Natronobacterium pharaonis:* Wavelength regulation by anions, *Biochemistry 33*, 6387−6393.
20. Bálint, Z., Lakatos, M., Ganea, C., Lanyi, J. K., and Váró, G. (2004) The nitrate transporting photochemical reaction cycle of the pharaonis halorhodopsin, *Biophys. J. 86*, 1655−1663.
21. Váró, G., Needleman, R., and Lanyi, J. K. (1995) Light-driven chloride transport by halorhodopsin from *Natronobacterium pharaonis.* 2. Chloride release an uptake, protein conformation change, and thermodynamics, *Biochemistry 34*, 14500−14507.
22. Ludmann, K., Ibron, G., Lanyi, J. K., and Váró, G. (2000) Charge motions during the photocycle of *pharaonis* halorhodopsin, *Biophys. J. 78*, 959−966.
23. Gerscher, S., Mylrajan, M., Hildebrandt, P., Baron, M.-H., Müller, R., and Engelhard, M. (1997) Chromophore-anion interaction in halorhodopsin from *Natronobacterium pharaonis* probed by time-resolved resonance Raman spectroscopy, *Biochemistry 36*, 11012−11020.
24. Shibata, M., Muneda, N., Sasaki, T., Shimono, K., Kamo, N., Demura, M., and Kandori, H. (2005) Hydrogen-bonding alterations of the protonated Schiff base and water molecules in the chloride pump of *Natronobacterium pharaonis*, *Biochemistry 44*, 12279−12286.
25. Hohenfeld, I. P., Wegener, A. A., and Engelhard, M. (1999) Purification of histidine tagged bacteriorhodopsin, *pharaonis* halorhodopsin, and *pharaonis* sensory rhodopsin II functionally expressed in *Escherichia coli*, *FEBS Lett. 442*, 198−202.
26. Losi, A., Wegener, A. A., Engelhard, M., and Braslavsky, S. E. (2001) Thermodynamics of the early steps in the photocycle of *Natronobacterium pharaonis* halorhodopsin. Influence of medium and anion substitution, *Photochem. Photobiol. 74*, 495−503.
27. Vogel, R., and Siebert, F. (2003) New insights from FTIR spectroscopy into molecular properties and activation mechanisms of the visual pigment rhodopsin, *Biospectroscopy 72*, 133−148.
28. Rödig, C., Chizhov, I. V., Weidlich, O., and Siebert, F. (1999) Time-resolved step-scan FTIR spectroscopy reveals differences between early and late M intermediates of bacteriorhodopsin, *Biophys. J. 76*, 2687−2701.
29. Fahmy, K., Grossjean, M. F., Siebert, F., and Tavan, P. (1989) The photoisomerization in bacteriorhodopsin studied by FTIR linear dichroism and photoselection experiments combined with quantumchemical theoretical analysis, *J. Mol. Struct. 214*, 257−288.
30. Sato, M., Kanamori, T., Kamo, N., Demura, M., and Nitta, K. Stopped-flow analysis on anion binding to blue-form halorhodopsin from *Natronobacterium pharaonis*: comparison with anion-uptake process during the photocycle, *Biochemistry* 2002.
31. Váró, G., Brown, L. S., Sasaki, J., Kandori, H., Maeda, A., Needleman, R., and Lanyi, J. K. (1995) Light-driven chloride transport by halorhodopsin from *Natronobacterium pharaonis*. 1. The photochemical cycle, *Biochemistry 34*, 14490−14499.
32. Kulcsár, A., Groma, G. I., Lanyi, J. K., and Váró, G. (2000) Characterizatiojn of the proton-transporting photocycle of pharaonis halorhodopsin, *Biophys. J. 79*, 2705−2713.
33. Heyde, M. E., Gill, D., Kilponen, R. G., and Rimai, L. (1971) Raman spectra of Schiff bases of retinal (models of visual photoreceptors), *J. Am. Chem. Soc. 93*, 6776−6780.
34. Ottolenghi, M. (1980) The Photochemistry of Rhodopsin, in *Advances in Photochemistry* (Pitts, J. N., Hammond, G. S., Gollnik, K., and Grosjean, D., Eds.) Vol. 12, pp 97−200, Wiley-Interscience, NY.
35. Barth, A. (2000) The infrared absorption of amino acid side chains, *Prog. Biophys. Mol. Biol. 74*, 141−173.
36. Rosenthal, M. R. (1973) The myth of the non-coordinating anion, *J. Chem. Educ. 50*, 331−335.
37. Nakamoto, K. (1986) *Infrared and Raman Spectra of Inorganic and Coordination Compounds*, John Wiley & Sons, NY.
38. Miller, F. A., and Wilkins, C. H. (1952) Infrared spectra and characteristic frequencies of inorganic ions, *Anal. Chem. 24*, 1253−1294.
39. Hein, M., Wegener, A. A., Engelhard, M., and Siebert, F. (2003) Time-resolved FTIR studies of sensory rhodopsin II (NpSRII) from *Natronobacterium pharaonis*: Implications for proton transport and receptor activation, *Biophys. J. 84*, 1208−1217.

40. Hein, M., Radu, I., Klare, J. P., Engelhard, M., and Siebert, F. (2004) Consequences of counterion mutation in sensory rhodopsin II of *Natronobacterium pharaonis* for photoreaction and receptor activation: An FTIR study, *Biochemistry 43*, 995−1002.
41. Váró, G., Zimányi, L., Fan, X., Sun, L., Needleman, R., and Lanyi, J. K. (1995) Photocycle of halorhodopsin from *Halobacterium salinarium*, *Biophys. J. 68*, 2062−2072.
42. Schobert, B., and Lanyi, J. K. (1982) Halorhodopsin is a light-driven chloride pump, *J. Biol. Chem. 257*, 10306−10313.
43. Bamberg, E., Hegemann, P., and Oesterhelt, D. (1984) Reconstitution of the light-driven electrogenic ion pump halorhodopsin in black lipid membranes, *Biochim. Biophys. Acta 773*, 53−60.
44. Brown, L. S., Needleman, R., and Lanyi, J. K. (1996) Interaction of proton and chloride transfer pathways in recombinant bacteriorhodopsin with chloride transport activity: Implication for the chloride translocation mechanism, *Biochemistry 35*, 16048−16054.

BI060753J